

# Study of the Different Transmission Line Faults for a Grid Connected Wind Farm with Different Types of Control Method for RSC

Reza Najafi

Electrical Engineer, 56517-65835 Germei, Ardabil, Iran  
Corresponding author, e-mail: reza.najafi1369@yahoo.com

## Abstract

Wind power stations, many located in remote areas; so they are characterized by weak grids and are often submitted to power system disturbance like faults. In this paper, the behaviour of a wind energy conversion system that uses the control of the rotor side converter (RSC) by three different methods under faulty conditions is presented. The behaviour of these systems during a grid failure is an important issue. DFIG is analysed and simulated under differing faulty conditions in the environment of MATLAB/SIMULINK. Simulation results show that the proposed method has proper operation during fault conditions.

**Keywords:** DFIG, Vector control, direct power control, combined vector and direct power control

Copyright © 2017 Institute of Advanced Engineering and Science. All rights reserved.

## 1. Introduction

Vector control is the most popular method used in the DFIG-based WTs [1]. Furthermore, the coefficients of proportional–integral (PI) controllers, in the conventional VC, should be optimally tuned to ensure the system stability within the whole operating range and achieve sufficient dynamic response during the transient conditions [2]. This will deteriorate the transient performance of VC and affect the system stability within changing operation conditions. To overcome the aforementioned problems, different nonlinear control procedures such as direct torque control/direct power control (DTC/DPC) have been proposed [3].

This paper presents the performance evaluation of Doubly-Fed Induction Generator Using Combined Vector Control and Direct Power Control Method. Combined vector and direct power control (CVDPC) is used for the rotor side converter (RSC) of double-fed induction generators (DFIGs). The control system is according a direct current control by selecting suitable voltage vectors from a switching table.

## 2. Different Control Method

### 2.1. Vector Control

The dynamic stator, active and reactive power equations of DFIG in a synchronously ( $\omega_s$ ) rotating d-q reference frame can be expressed by the following equations [4]:

$$P_s = \frac{3}{2} (V_{ds} I_{ds} + V_{qs} I_{qs}) \quad (1)$$

$$Q_s = \frac{3}{2} (V_{qs} I_{ds} - V_{ds} I_{qs}) \quad (2)$$

The stator voltage vector is aligned with the d axis, therefore, is equal to zero, and so the stator active and reactive power equation is simplified:

$$P_s = \frac{3}{2} V_{ds} I_{ds} \quad (3)$$

$$Q_s = -\frac{3}{2} V_{ds} I_{qs} \tag{4}$$

**2.2. Direct Power Control**

The equations of active and reactive power in DPC method can be expressed as follows [5]:

$$P_s = \frac{3}{2} \frac{L_m}{\sigma L_s L_r} \omega_s |\vec{\lambda}_s| |\vec{\lambda}_r| \sin \delta \tag{5}$$

$$Q_s = \frac{3}{2} \frac{\omega_s}{\sigma L_s} |\vec{\lambda}_s| \left[ \frac{L_m}{L_r} |\vec{\lambda}_s| - |\vec{\lambda}_r| \cos \delta \right] \tag{6}$$

$$\delta = \rho_s - \theta_r \tag{7}$$

Where  $L_s, L_r$  are the stator and rotor self-inductance,  $L_m$  is the mutual-inductance,  $\sigma$  is leakage coefficient,  $\omega_s$  is the stator angular frequency,  $\delta$  is the angle between the stator and rotor flux linkage space vector,  $P_s$  and  $\theta_r$  are the angle between  $\sigma$  axis (rotating at electrical angular speed of the rotor  $\omega_m$ ) and their flux linkage as shown in Figure 1  $\lambda_s$  and  $\lambda_r$  are the stator and rotor flux linkage.

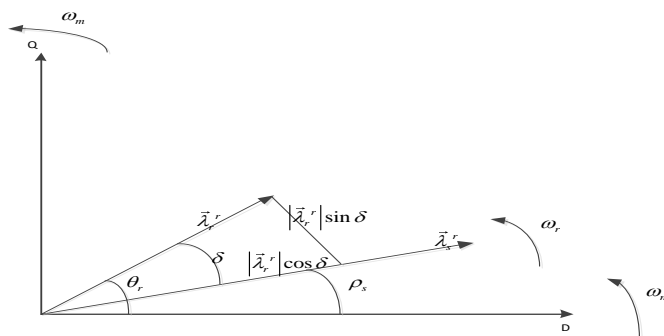


Figure 1. Flux space vector in rotor reference frame (OQ)

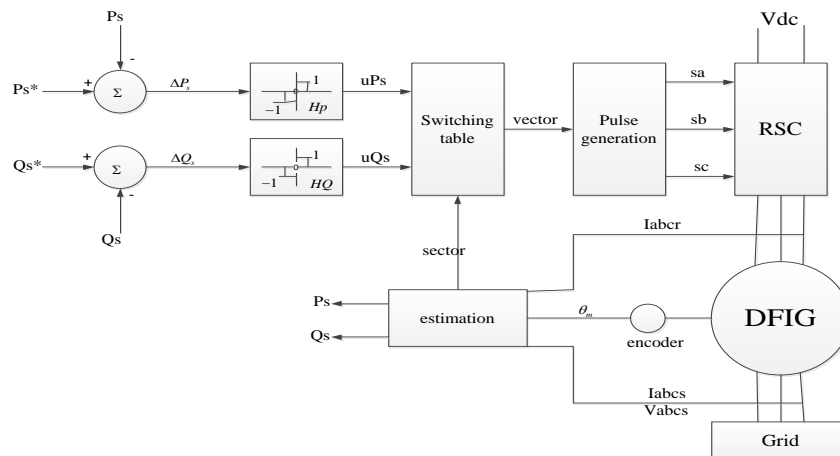


Figure 2. Block diagram of a DPC for DFIG

The stator windings of DFIG are directly connected to the grid. So under normal conditions, the stator voltage is constant and by neglecting the stator resistance; the stator flux linkage is constant too, so the stator active and reactive power can be written as:

$$P_s = A \left| \tilde{\lambda}_r \right| \sin \delta \quad (8)$$

$$Q_s = B \left[ C - \left| \tilde{\lambda}_r \right| \cos \delta \right] \quad (9)$$

Where A, B and C are constant value. From the above equations, it can be seen stator active power is related to magnitude of rotor flux linkage and sinus of the angle between the stator and rotor flux linkage, as well stator reactive power is related to magnitude of rotor flux linkage and Cosine of the angle between stator and rotor flux linkage, as shown in Figure 1. In direct power control, the stator active and reactive power directly controlled by comparing the reference power with estimated power. The power error is compared with a hysteresis band wide and flags of the hysteresis band wide are specified. The block diagram of this method is shown in Figure 1. Optimal voltage vector can be selected by Knowing rotor flux sector, and the flags of hysteresis comparators. This optimal switching table is shown in Table 1. For example, if the rotor flux linkage vector located in sector I and v2 selected, this voltage vector makes active and reactive power to decrease (the active power will be more negative) and if V3 selected, makes the active power to decrease and reactive power to increase.

### 2.3. Proposed Combined Vector Control and Direct Power Control

Due to the vector control, a phase locked loop (PLL) for the stator voltage used, therefore the stator voltage space vector gets along the d axis that rotates at slip speed in the d-q reference frame. So, by neglecting the stator resistance, the stator flux linkage space vector lags the stator voltage space vector by 90 degrees. The location of stator voltage vector and d-q axis in the d-q reference frame is shown in Figure 3 [6].

Table 1. Switching table for DPC method

		1	2	3	4	5	6
1	1	V5	V6	V1	V2	V3	V4
	0	V0	V7	V0	V7	V0	V7
	-1	V3	V4	V5	V6	V1	V2
-1	1	V6	V1	V2	V3	V4	V5
	0	V0	V7	V0	V7	V0	V7
	-1	V2	V3	V4	V5	V6	V1

Due to the equations (8) and (9), the related variations of active power and reactive power are shown by red lines in Figure 3. As shown in this figure, variation of active power is along the d axis, and the variation of reactive power is along the q axis. From equation (3) and (4) and Figure 1, it is concluded:

$$\begin{aligned} \Delta P_s &\propto \Delta I_{ds} \\ \Delta Q_s &\propto -\Delta I_{qs} \end{aligned} \quad (10)$$

It means that the variation of active power is proportional to the variation of d axis stator current and variation of reactive power is proportional to negative variation of q axis stator current. So, d-q axis stator currents can be directly controlled like DPC by a switching table. However, because of the negative relative of reactive power and q axis stator current, the switching table became as Table 2. Figure 4 shows the block diagram of the proposed method which the d--q axis stator currents errors have been compared with a hysteresis band wide. The flags of this comparator and the sector of rotor flux select the voltage vector from Table 2.

**2.4. The Control Methods of Rotor Side Converter and Grid Side Converter for DFIG**

Direct power control of voltage source converters has been introduced in [6]. The injected or absorbed Active and reactive power of a voltage source converter directly control by this method. The main idea of this method is like DPC for rotor side converter.

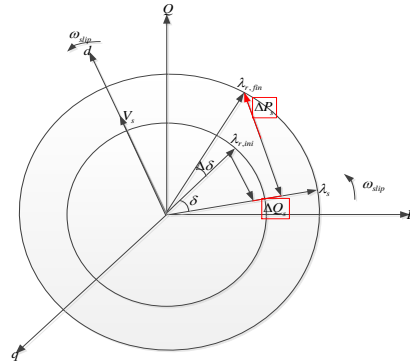


Figure 3. Stator voltage and flux in DQ reference frame and the relation of direct power to d-q axis currents

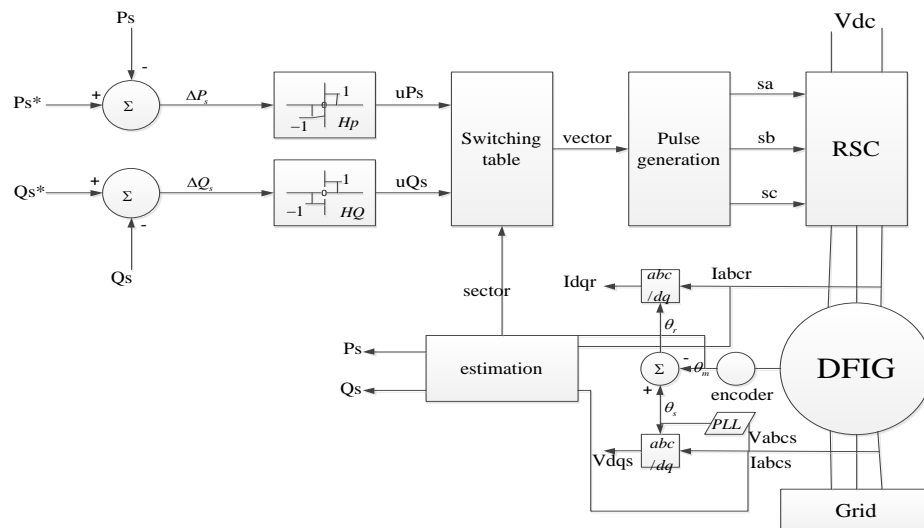


Figure 4. The block diagram of proposed method for RSC

Table 2. Switching table of proposed method for RSC

		1	2	3	4	5	6
1	1	V6	V1	V2	V3	V4	V5
	0	V0	V7	V0	V7	V0	V7
	-1	V2	V3	V4	V5	V6	V1
-1	1	V5	V6	V1	V2	V3	V4
	0	V0	V7	V0	V7	V0	V7
	-1	V3	V4	V5	V6	V1	V2

**3. Results and Discussion**

**3.1. Single-line to Ground Fault**

In this part, the impact of voltage sags resulting from a remote fault on the 25 KV system can be seen. In this simulation the mode of operation is initially Var regulation with

$Q_{ref}=0$  and the wind speed is constant at 8 m/s. To implement the line fault a single phase to ground fault is implemented on the 25 KV line. The fault occurs for a period of 9 cycles at  $t=0.2$  seconds. The results of the simulation are shown in Figure 5 and Figure 6. Stator voltage and electromagnetic torque waveforms for all three methods were obtained and compared.

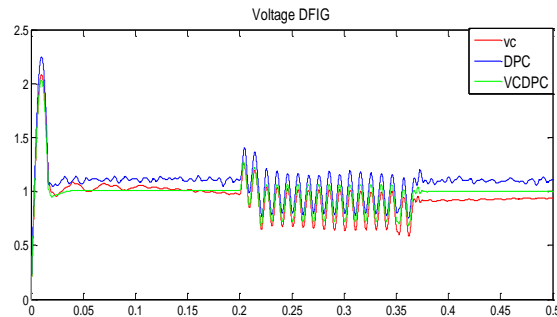


Figure 5. Stator voltage of DFIG in three different methods

In Figure 5 positive sequence voltage at wind turbine terminals for different methods is shown. According to the results of the simulation can be concluded that the voltage waveform of the proposed method than other methods contains is waveform stable. In addition, the proposed method than other methods after clearing the fault is faster retrieval. Numerical comparisons are shown in the table below.

Table 3. Comparing the methods

	Before fault	After fault
<b>VC</b>	0.98	0.907
<b>DPC</b>	1.1	1.09
<b>VCDPC</b>	1	1

In Figure below electromagnetic torque for three different methods shown.

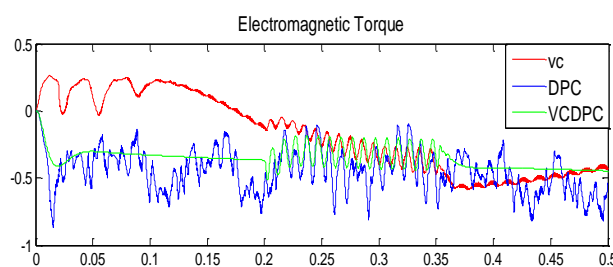


Figure 6. Electromagnetic torque in three different methods

### 3.2. Double Lines to Ground Fault

Similar previous state, voltage and torque waveform for two lines to ground fault has been achieved. As shown in Figure 7 and Figure 8. Numerical comparisons are shown in the Table 4.

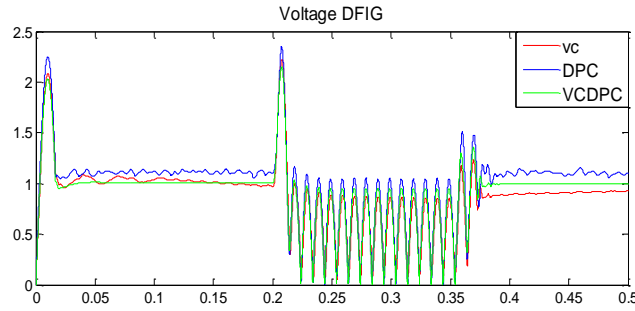


Figure 7. Stator voltage of DFIG in three different methods

Table 4. Comparison the methods

	Before fault	After fault
<b>VC</b>	0.99	0.9
<b>DPC</b>	1.1	1.09
<b>VCDPC</b>	1	1

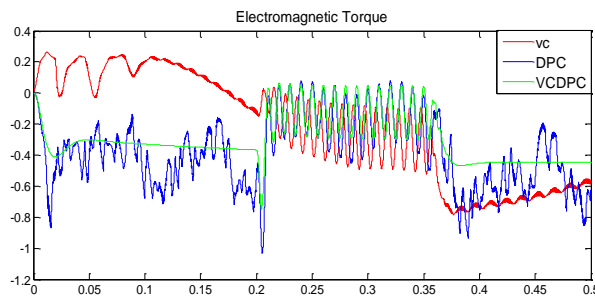


Figure 8. Electromagnetic torque in three different methods

**3.3. Three Lines to Ground Fault**

Similar previous state, voltage and torque waveform for three lines to ground fault has been achieved. As shown in Figure 9 and Figure 10. Numerical comparisons are shown in the Table 5.

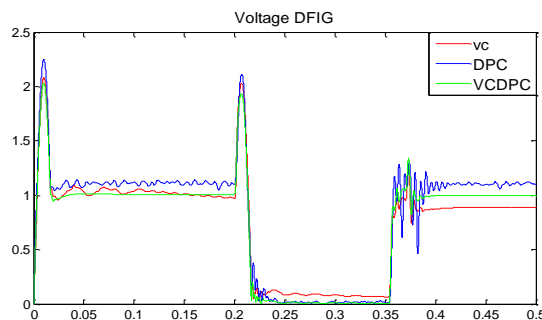


Figure 9. Stator voltage of DFIG in three different methods

Table 5. Comparing the methods

	Before fault	After fault
<b>VC</b>	0.98	0.88
<b>DPC</b>	1.1	1.1
<b>VCDPC</b>	1	1

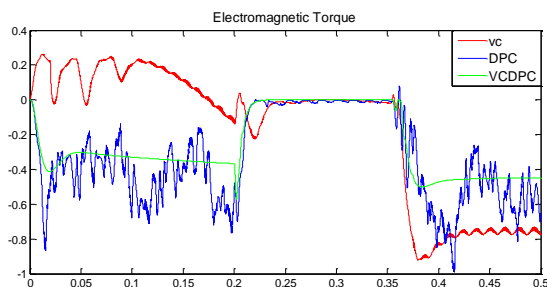


Figure 10. Electromagnetic torque in three different methods

#### 4. Conclusion

In this paper a wind generation system based on DFIG under power system disturbance has been simulated and an appropriate controller is designed to control the reactive power to the grid and help in grid improvement. By as the generator and converter connected, the synchronism of operation remains established during and after the faulty operation can be continued immediately after the fault has been cleared. Suitable controller designed is adopted to improve the transient and dynamic performance of DFIG under these unusual grid conditions. This paper analyses the DFIG transient behaviour and control possibility under grid disturbances like fault. In this paper, with the help of only one rotor side converter we are able to control the reactive power and maintain the stability of the grid under faulty conditions.

#### References

- [1] S Li, TA Haskew, KA Williams, RP Swatloski. Control of DFIG wind turbine with direct-current vector control configuration. *IEEE Trans. Sustain. Energy*. 2012; 3(1): 1-11.
- [2] L Xu, P Cartwright. Direct active and reactive power control of DFIG for wind energy generation. *IEEE Trans. Energy Convers*. 2008; 21(3): 750-758.
- [3] J Hu, H Nian, B Hu, Y He. Direct active and reactive power regulation of DFIG using sliding-mode control approach. *IEEE Trans. Energy Convers*. 2009; 25(4): 1028-1039.
- [4] R Pena, JC Clare, GM Asher. *Doubly fed induction generator using back-to-back PWM converters and its application to variable speed wind-energy generation*. Inst. Electr. Eng. Proc. Elect. Power Appl. 1996; 143(3): 231-241.
- [5] J Mohammadi, S Vaez-Zadeh, S Afsharnia, E Daryabeigi. A Combined Vector and Direct Power Control for DFIG-Based Wind Turbines. *IEEE Trans. Sustainable Energy*. 2015; 5(3): 760-775.
- [6] ME Zarei, B Asaei. *Combined Vector Control and Direct Power Control Methods for DFIG under Normal and Unbalanced and Distorted Grid Voltage Conditions*. 4th Power Electronics, Drive Systems & Technologies Conference (PEDSTC2013). Tehran, Iran. 2013.

#### Appendix 1

Parameters of the simulated DFIG:

Rated power: 2MW

Rated voltage (phase to phase): 690 v

Stator resistance ( $R_s$ ): 1.162 m $\Omega$

Rotor resistance ( $R_r$ ): 1.3072 m $\Omega$

Stator inductance ( $L_s$ ): 3.1 mH

Rotor inductance ( $L_r$ ): 3.1 mH

Mutual inductance ( $L_m$ ): 3mH

Number of pole (P): 4

DC link capacitor ( $C_f$ ): 16000 $\mu$ F

Grid frequency: 50 Hz